Numerical Simulation of the Coffee-ring Effect Inside Containers with Time-dependent Evaporation Rate

Hyundong Kim
Korea University - Seoul Campus: Korea University
Junxiang Yang
Korea University - Seoul Campus: Korea University
Sangkwon Kim
Korea University - Seoul Campus: Korea University
Chaeyoung Lee
Korea University - Seoul Campus: Korea University
Sungha Yoon
Korea University
Soobin Kwak
Korea University - Seoul Campus: Korea University
Junseok Kim (cfdkim@korea.ac.kr)
Korea University - Seoul Campus: Korea University https://orcid.org/0000-0002-0484-9189

Research Article

Keywords: Stripe formation , Time-dependent evaporation rate , Coffee-ring effect

Posted Date: May 20th, 2021

DOI: https://doi.org/10.21203/rs.3.rs-476882/v1

Version of Record: A version of this preprint was published at Theoretical and Computational Fluid Dynamics on January 6th, 2022. See the published version at https://doi.org/10.1007/s00162-021-00602-x.

manuscript No.
(will be inserted by the editor)

Numerical simulation of the coffee-ring effect inside containers with time-dependent evaporation rate

Hyundong Kim[1] · **Junxiang Yang**[1] · **Sangkwon Kim**[1] · **Chaeyoung Lee**[1] · **Sungha Yoon**[1] · **Soobin Kwak**[1] · **Junseok Kim**[1]

Received: 29 April 2021

Abstract In this work, using a mathematical model and numerical simulation, we investigate the effect of time-dependent evaporation rates on stripe formation inside containers, which is driven by the coffee-ring effect. The coffee particles inside a container move according to random walk and under the gravitational force. Because of the non-uniform evaporation rate, we can observe stripe formation inside a container filled with liquid carrying coffee particles. We perform various numerical experiments to demonstrate the proposed model can simulate the stripe formation in a container.

Keywords Stripe formation · Time-dependent evaporation rate · Coffee-ring effect

H. Kim
rlagusehd@korea.ac.kr

J. Yang
nexusxiang@outlook.com

S. Kim
ksk8863@korea.ac.kr

C. Lee
chae1228@korea.ac.kr

S. Yoon
there122@korea.ac.kr

S. Kwak
soobin23@korea.ac.kr

J. Kim
Tel.: +82-2-3290-3077
Fax: +82-2-929-8562
cfdkim@korea.ac.kr
[1] Department of Mathematics, Korea University, Seoul 02841, Republic of Korea

1 Introduction

When a drop of coffee evaporates on a solid substrate, the coffee particles form a ring-like stain at the contact line. This phenomenon is a consequence of faster evaporation at the contact line, driving the coffee particles to convectively migrate toward the contact lines [1], which is known as the coffee-ring effect [2–4]. The physical phenomenon related to the coffee-ring effect has been researched in several experiments withal various colloidal suspensions containing nanoparticles [5–10], air bubbles [11], quantum dots [12–14], biological fluids [15–21], bacteria [22–24]. Expanding the definition of the coffee-ring effect, liquid-liquid coffee-ring effect is considered which taking into account systems without involving any evaporation [25]. In quite a few industrial and scientific fields, the physics similar to the coffee-ring effect is one of the most significant issues in controlling the distribution of the solute in a solution during evaporating process. Analyzing and understanding the process of ring formation can be technologically profound for those who want to tame advantage of or suppress the coffee-ring effect. There are many physical applications by using the principle of coffee-ring effect, such as ink-jet printing [26–32], making cyrstal morphologies [33], central spot formation in droplets [34], uniform droplet printing of graphene micro-rings [35], converting colour to length for quantitative immunoassays using a ruler as readout [36], phase separation effects of medium and high-molecular-weight polymers [37], pesticide spray application [38], micro-technologies in biological field [39–41] and coatings [42, 43]. For more review on the principles and applications of the sessile drop evaporation and coffee-ring effect, see [44, 45]. The coffee-ring effect has also been investigated in various numerical experiments based on the Monte Carlo method [46–50], finite element method [51, 52] or finite difference method [53].

The objective of the present work is to suggest the mathematical model without the capillary flow that focuses on investigating a diffusion process of the Brownian particles under gravitational force and to perform various numerical experiments to demonstrate the proposed model can simulate the coffee-ring effect inside containers with time-dependent evaporation rate. The proposed method is based on the Monte Carlo method.

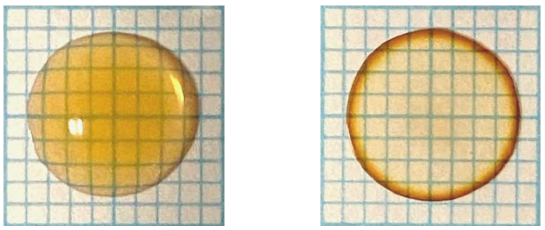

(a) (b)

Fig. 1 Coffee droplet on a transparent film on a grid paper (a) before and (b) after evaporation.

Figure 1(a) and (b) show coffee droplet on a transparent film on a grid paper before and after evaporation. After evaporation of coffee droplet, we can observe coffee stain and coffee-ring.

(a) (b)

Fig. 2 Making coffee angel rings in a conical flask: (a) Coffee solution contained in a conical flask and (b) Coffee angel rings made after evaporation.

Figure 2 shows making coffee angel ring in a conical flask. Figure 2(a) is a photograph of coffee solution contained in a conical flask. The coffee angel ring made by evaporating can be seen in Fig. 2(b). As we can see in Fig. 2(b), a pattern of coffee angel ring becomes repeatedly thicker and lighter. Main mechanisms for forming these coffee rings are periodically chaining room temperature and humidity, i.e., changing evaporation rates.

The paper is organized as follows. In Section 2, we present the governing equation and the numerical solution algorithm. The numerical results are presented in Section 3. Finally, conclusions are drawn in Section 4.

2 Governing equation and numerical solution algorithm

Let Ω_t be a time-dependent liquid domain at time t in a solid container. The time-dependent liquid domain Ω_t is presented by a level-set function $\phi(\mathbf{x}, t)$, i.e., $\Omega_t = \{\mathbf{x} \in \mathbb{R}^3 | \phi(\mathbf{x}, t) > 0\}$. Let Γ_t be the liquid surface at time t contacting the air. The liquid domain contains the coffee particles which are defined as the Lagrangian points moving under Brownian motion and gravitational force. Figure 3 depicts a time-dependent liquid domain Ω_t including coffee particles and a top-level surface of liquid domain Γ_t with the scalar field ϕ.

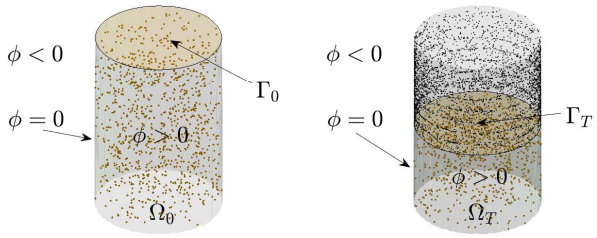

(a) (b)

Fig. 3 Schematic illustration of the liquid domain Ω_t over time at (a) $t = 0$ and (b) $t = T$ where T is a certain time. Note that the coloured surface represents the top-level surface Γ_t.

For the sake of simplicity of modeling, we assume coffee particles have only mass and no volume and the fluid surface moves under the time-dependent evaporation rates. Assuming that the force on the particle is zero, the governing equation can be derived from the Langevin equation [53]:

$$\frac{d\mathbf{X}}{dt} = \frac{\alpha}{\sqrt{dt}}\boldsymbol{\psi}(\mathbf{X}) + \mathbf{g} \text{ on } \Omega_t, \tag{1}$$

where $\mathbf{X}$ is Lagrangian variable for a particle, t is time, $\mathbf{g} = (0, 0, -g)$ is the scaled gravitational force. Here, $\boldsymbol{\psi}(\mathbf{X}) = (\rho\cos(\theta)\sin(\varphi),\ \rho\sin(\theta)\sin(\varphi),\ \rho\cos(\varphi))$ represents random force of Brownian particle, where ρ is a random variable with the probability density function $f(\rho) = e^{-0.5\rho^2}/\sqrt{2\pi}$ and between $[-3,\ 3]$ which is 99.998% confidence interval. The random variables θ and φ are uniformly distributed on the interval $[0,\ \pi]$. Using the explicit Euler's method, we discretize Eq. (1) as

$$\frac{\mathbf{X}_k^{n+1} - \mathbf{X}_k^n}{\Delta t} = \frac{\alpha}{\sqrt{\Delta t}}\boldsymbol{\psi}(\mathbf{X}_k^n) + \mathbf{g},\ \ k = 1, 2, \ldots, N_k, \tag{2}$$

where $\mathbf{X}_k^n$ is the k-th particle position at time $t = n\Delta t$, Δt is the time step and N_k is the total number of particles. Equation (2) can be rewritten as

$$\mathbf{X}_k^{n+1} = \mathbf{X}_k^n + \alpha\sqrt{\Delta t}\boldsymbol{\psi}(\mathbf{X}_k^n) + \Delta t\mathbf{g},\ \ k = 1, 2, \ldots, N_k \tag{3}$$

We assume that the $n+1$ time-level particle is $\mathbf{X}_k^{n+1} = (X_k^{n+1}, Y_k^{n+1}, Z_k^{n+1})$. Every particle is pinned if it satisfies the following conditions: (i) $\phi(\mathbf{X}_k^{n+1}) < 0$, (ii) $Z_k^{n+1} > S(t)$ where $S(t)$ is the position of the liquid surface at time

$t = n\Delta t$, and (iii) $\Phi(\mathbf{X}_k^{n+1}) < 0$ where $\Phi(\mathbf{x}, t)$ represents a level-set of domain. If a particle goes outside the liquid domain ($\phi < 0$), then the particle moves to the crossing point of $\phi(\mathbf{x}, t) = 0$. The pinning process of these conditions is schematically represented in Fig. 4. If the particle satisfies the pinning conditions, then it is pinned like a diamond symbol. If the pinning conditions are not satisfied and $\phi < 0$, then the particle moves to $\phi = 0$, such as the square symbol and triangle symbol.

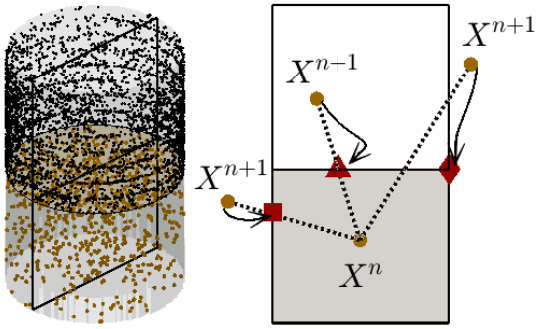

Fig. 4 Schematic representation of pinning process.

3 Numerical experiments

Unless otherwise noted, $z = S(t)$ is the position of the liquid surface at time t, N is the number of particles except pinned particles, the total number of particles N_k is set to 5×10^5, and the size of bins in the histograms is set to 0.03 in this study.

3.1 Particle motion except evaporation

We first perform the numerical simulation to confirm the motion of particles without any evaporation in a cylindrical container. The static liquid domain is defined as $\Omega_t = \{\mathbf{x} \in \mathbb{R}^3 | \phi(\mathbf{x}, t) > 0\}$:

$$\phi(x, y, z, t) = \begin{cases} 1 - \sqrt{x^2 + y^2} & \text{if } 0 \le z \le S(t), \\ -1 & \text{otherwise,} \end{cases}$$

where $S(t) = 3$ is the position of the liquid surface at time t. The gravity $\mathbf{g} = (0, 0, -4)$, the temporal step size $\Delta t = 0.0001$ and $\alpha = 1$ are used. The total number of particles is 100000. The evolution of particles in a cylindrical container without evaporation can be seen in Figure 5(a). The number of particles with respect to height is shown in Fig. 5(b). As can be shown from the histogram in Fig. 5(b), the number of particles increases at the lower height of cylinder over time, therefore we can confirm that the particles are stacking to the bottom of the cylinder by the gravitational force.

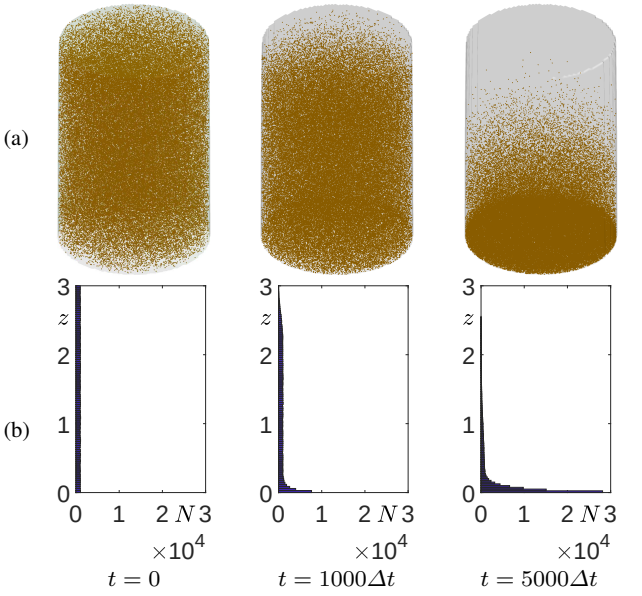

Fig. 5 (a) Evolution of particles in a cylindrical container without evaporation. (b) Histograms of particle number with respect to height at the corresponding times.

3.2 Coffee-ring formation on constant evaporation rate

We also define the time-dependent liquid domain as follows.

$$\phi(x, y, z, t) = \begin{cases} 1 - \sqrt{x^2 + y^2} & \text{if } 0 \le z \le S(t), \\ -1 & \text{otherwise,} \end{cases}$$

where $S(t) = 3 - 0.125t$ is the position of the liquid surface at time t. We use $\mathbf{g} = (0, 0, -0.1)$, $\Delta t = 0.0001$ and $\alpha = 1$. Figure 6(a) shows the evolution of particles in a cylindrical container. The number of pinned particles is shown in Fig. 6(b), as the height of liquid interface moves from 3 to 0 over time. As can be observed from the histogram in Fig 6(b), the number of pinned particles decreases around the cylinder height 3 to 2.5, and the number of particles increases around the cylinder height 2.5 to 0.

3.3 Coffee-ring formation on changing evaporation rate

Using the proposed method, we perform the numerical simulation for the stripe pattern formation in a cylindrical container with the time-dependent evaporation rate. The time-dependent liquid domain is defined as follows.

$$\phi(x, y, z, t) = \begin{cases} 1 & \text{if } \sqrt{x^2 + y^2} \le 1 \text{ and } 0 \le z \le S(t), \\ -1 & \text{otherwise,} \end{cases}$$

where $S(t^{n+1}) = S(t^n) - \Delta t(A + \beta(\sin(\gamma n \Delta t) + 1))$ with $S(0) = 3$. Here, the superscript n represents the value at n-time level. We set $\mathbf{g} = (0, 0, -4)$, $\Delta t = 0.0001$, $A = 0.01$, $\alpha = 1$, $\beta = 1$ and $\gamma = 10\pi$. The first column of Fig. 7 shows the initial state. From the second column to the

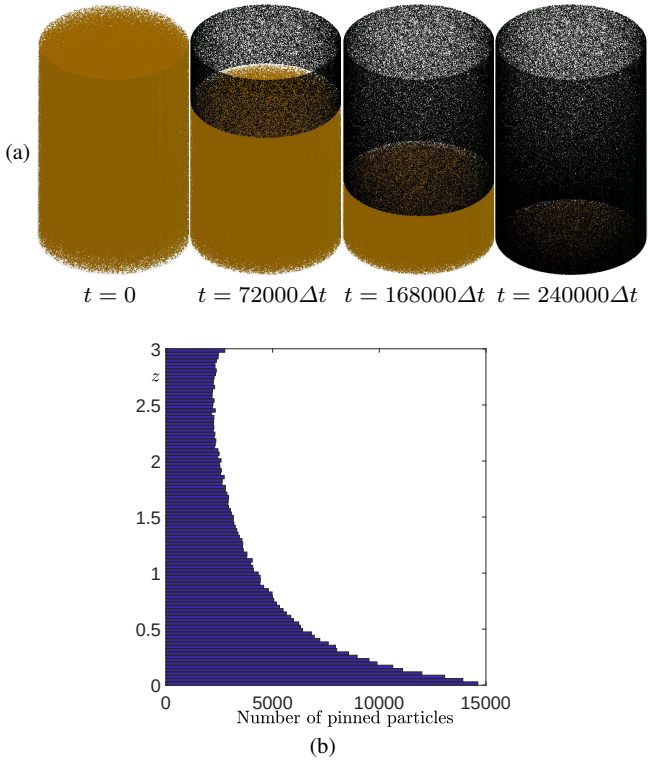

Fig. 6 (a) Evolution of particles in a cylindrical container. (b) Histogram of pinned particles with respect to height at final time $t = 240000\Delta t$.

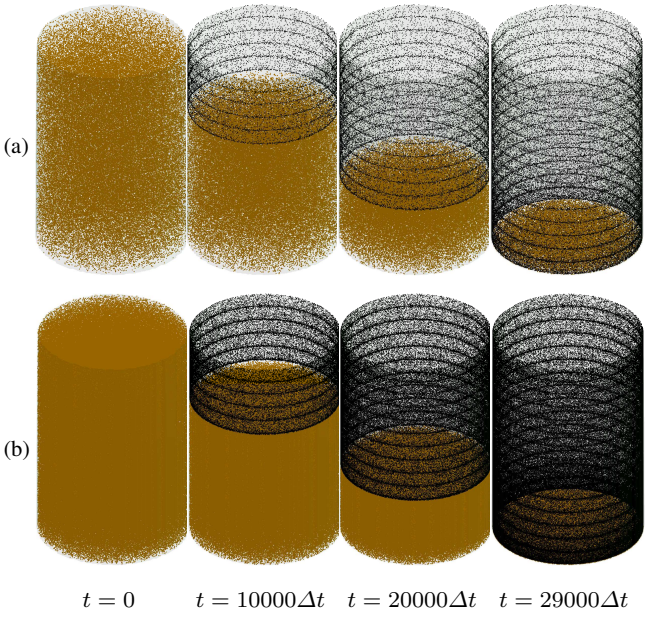

Fig. 7 Evolution of particles on the time-dependent evaporation rate in a cylindrical container: the number of particles is (a) 100000 and (b) 500000.

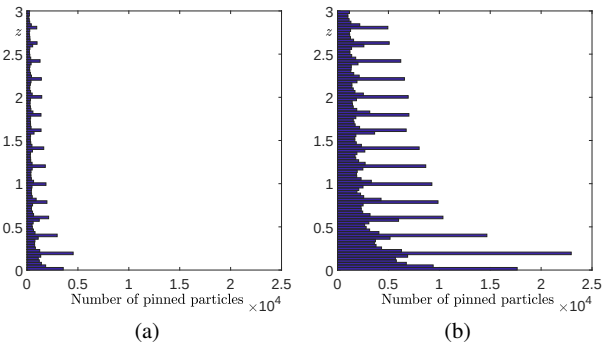

Fig. 8 Histogram of particles with respect to height at final time $t = 29084\Delta t$. The number of particles is (a) 100000 and (b) 500000.

fourth column in Fig. 7 describe the evolution of particles for the coffee-ring effect with respect to the number of particles, in a cylindrical container. Figure 8 shows the number of coffee particles as the liquid interface moves from 3 to 0 height over time. From left to right, the times are $t = 0$, $10000\Delta t$, $20000\Delta t$, and $29000\Delta t$. The number of particles is (a) 100000 and (b) 500000. From this numerical experiment, we can observe that coffee angel rings are clearly formed as the number of particles increases.

The number of pinned particles is decreasing and then increasing periodically as the height approach the bottom of the cylinder, and the number of particles is increasing rapidly where the stripe pattern is formed as shown in the histograms of Fig. 8.

3.4 Effect of container shape

To validate the effect of a container shape, we implement the numerical test for the stripe pattern formation in a conical container with the time-dependent evaporation rate using the proposed method. The time-dependent liquid domain is defined as

$$\phi(x,y,z,t) = \begin{cases} 1 & \text{if } \sqrt{x^2+y^2} \le z/3 \text{ and } 0 \le z \le S(t), \\ -1 & \text{otherwise,} \end{cases}$$

where $S(t^{n+1}) = S(t^n) - \Delta t(A + \beta(\sin(\gamma n \Delta t) + 1))$ with $S(0) = 3$. We select $\mathbf{g} = (0, 0, -4)$, $\Delta t = 0.0001$, $A = 0.01$, $\alpha = 1$, $\beta = 1$ and $\gamma = 10\pi$. In Fig. 9, we can see that the number of pinned particles becomes similar at each certain part of height of the conical container. Therefore, we can make conjecture that there is a container shape, time-dependent evaporation rate and gravitational force where the number of particles becomes similar anywhere when the stripe pattern is formed without capillary flow.

3.5 Effect of gravitational parameter

We investigate the effect of gravitational parameter on the formation of coffee ring in a $45°$ tilted cylinder. The time-dependent liquid domain is defined as

$$\phi(x,y,z,t) = \begin{cases} 1 & \text{if } \sqrt{x^2+y^2} \le 1 \text{ and } 0 \le z \le S(t), \\ -1 & \text{otherwise,} \end{cases}$$

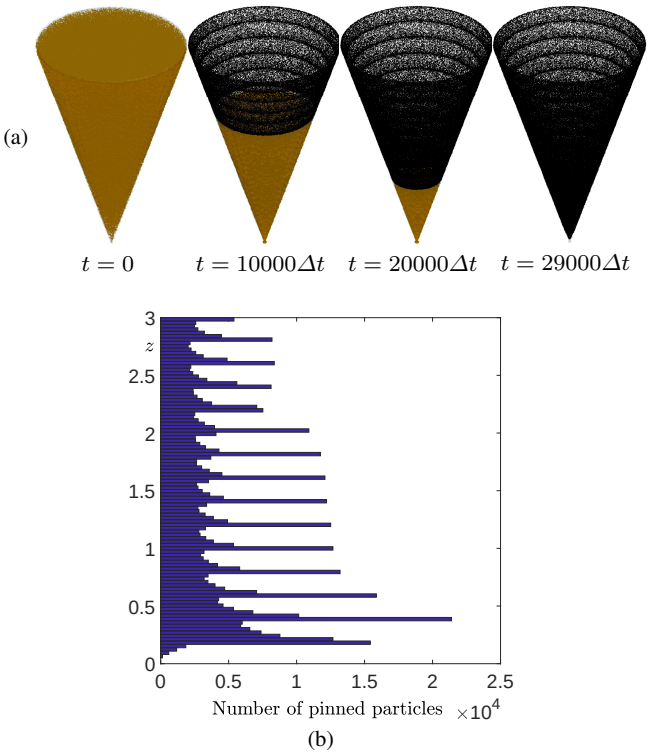

Fig. 9 (a) Evolution of particles on the time-dependent evaporation rate in a conical container. (b) Histogram of particles with respect to height at final time $t = 29084\Delta t$

where $S(t^{n+1}) = S(t^n) - \Delta t(A + \beta(\sin(\gamma n \Delta t) + 1))$ with $S(0) = x$. The gravitational force can be written as $\mathbf{g} = (g\sin(\theta), 0, -g\cos(\theta))$, where $\theta = 45^\circ$ is the tilted angle. In this simulation, we fix the parameters as $\Delta t = 0.0001$, $A = 0.01$, $\alpha = 2$, $\beta = 1$ and $\gamma = 20\pi$. Two different gravitational parameters are used as $g = 2$ and 4. Figure 10(a) and (b) show the snapshots of evolution from left to right $t = 0, 1000\Delta t, 2000\Delta t$, and $3000\Delta t$ with respect to $g = 2$ and 4, respectively. As we can observe, a smaller gravitational parameter drives the coffee particles settle slower and more particles are pinned on the side of wall boundary. On the other hand, a larger value of gravitational parameter causes the coffee particles settle faster and the number of pinned particles on both sides of wall boundary is relatively small. Around the bottom of the container, we can also see that the coffee particles are more gathered in the tilted direction under the influence of gravity.

3.6 Effect of tilt angle

Now, we shall perform the numerical simulation to observe the formation of coffee ring with respect to tilt angle. The numerical results in a 45° tilted cylinder are shown in Fig. 10(b). Here, we set a 30° tilted cylinder and the time-dependent

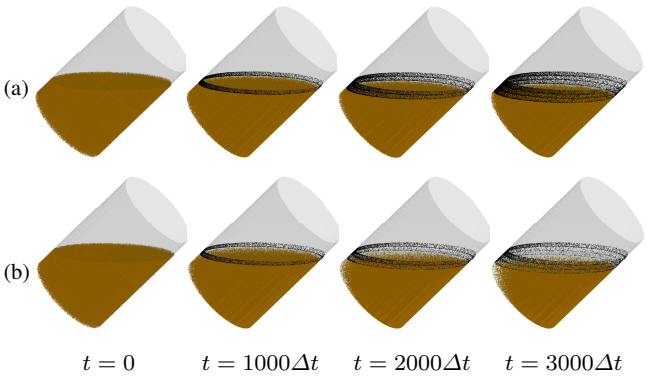

Fig. 10 Effect of gravitational parameter on the formation of coffee ring with (a) $g = 2$ and (b) $g = 4$.

liquid domain as follows.

$$\phi(x, y, z, t) = \begin{cases} 1 & \text{if } \sqrt{x^2 + y^2} \le 1 \text{ and } 0 \le z \le S(t), \\ -1 & \text{otherwise,} \end{cases}$$

where $S(t^{n+1}) = S(t^n) - \Delta t(A + \beta(\sin(\gamma n \Delta t) + 1))$ with $S(0) = \frac{1}{\sqrt{3}}x$. For $\theta = 30^\circ$, the gravitational force set to $\mathbf{g} = (g\sin(\theta), 0, -g\cos(\theta))$. In this experiment, the same values as the parameters set in Fig. 10(b) are used. Comparing the results between Fig. 10(b) and Fig. 11, we can see that the coffee ring formation in a 30° tilted cylinder is formed thicker on the right-side contact wall of the cylinder.

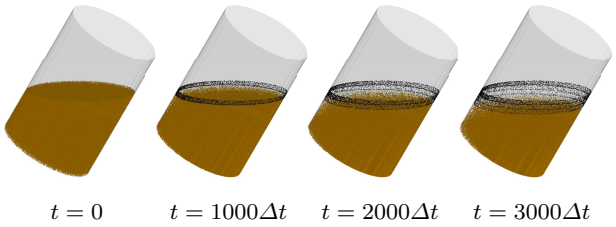

Fig. 11 Evolution of particles on a time-dependent evaporation rate in a 30° tilted cylinder.

Figure 12 shows histograms of number of pinned particles with respect to height at final time $t = 3000\Delta t$ in (a) a 45° tilted cylinder and (b) a 30° tilted cylinder. The histogram shown to the left position is the number of pinned particles in the area $x < 0$. Likewise, The histogram displayed to the right position is the number of pinned particles in the area $x > 0$. As can be clearly observed in the histograms of Figs. 12(a) and (b), as the angle of inclination decreases, the number of particles pinning on the right contact wall increases. Oppositely, around the boundary of the left contact wall, coffee particles slide along the direction of gravitational force, which does not stick well to the left contact wall, and then fall into the fluid, decreasing the number of particles that are pinned to the left contact wall.

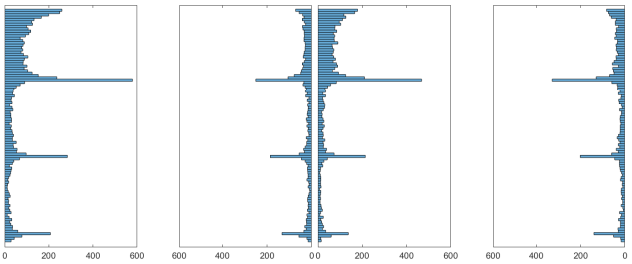

(a) (b)

Fig. 12 Histograms of number of pinned particles with respect to height at final time $t = 3000\Delta t$ in (a) 45° tilted and (b) 30° tilted cylinders.

4 Conclusions

We proposed the mathematical model for the stripe formation in a cup of coffee with time-dependent evaporation rates. Assuming that the force on the particle is zero, the governing equation could be derived from the Langevin equation. The time-dependent liquid domain Ω_t and liquid surface Γ_t are defined. Furthermore, using the Monte Carlo method, the coffee particles are defined as Lagrangian points moving under Brownian dynamics and gravity. We found the numerical solution of the governing equation using the explicit Euler's method. The numerical simulations are performed in the three-dimensional space. From the numerical results, we investigated that the distribution of particles and stripe pattern formations depend on the evaporation rates, the shape of container, the gravitational force and the tilt of the cylinder.

Acknowledgment

The first author (Hyundong Kim) was supported by Basic Science Research Program through the National Research Foundation of Korea (NRF) funded by the Ministry of Education (NRF-2020R1A6A3A13077105). Junxiang Yang was supported by China Scholarship Council (201908260060). Chaeyoung Lee was supported by Basic Science Research Program through the National Research Foundation of Korea (NRF) funded by the Ministry of Education (NRF-2019 R1A6A3A13094308). The corresponding author (Junseok Kim) was supported by Basic Science Research Program through the National Research Foundation of Korea (NRF) funded by the Ministry of Education (NRF-2019R1A2C1003053).

Declarations

Conflict of interest

The authors declare that there is no conflict of interests regarding the publication of this paper.

Data availability

The datasets generated during and/or analysed during the current study are available from the corresponding author on reasonable request.

References

1. Al-Milaji, K.N., Secondo, R.R., Ng, T.N., Kinsey, N., Zhao, H.: Interfacial Self-Assembly of Colloidal Nanoparticles in Dual-Droplet Inkjet Printing. Adv. Mater. Interf. 5, 1701561 (2018)
2. Deegan, R.D., Bakajin, O., Dupont, T.F., Huber, G., Nagel, S.R., Witten, T.A.: Capillary flow as the cause of ring stains from dried liquid drops. Nature 389(6653), 827–829 (2018)
3. Deegan, R.D., Bakajin, O., Dupont, T.F., Huber, G., Nagel, S.R., Witten, T.A.: Contact line deposits in an evaporating drop. Phys. Rev. E. 62(1), 756 (2000)
4. Yunker, P.J., Still, T., Lohr, M.A., Yodh, A.G.: Suppression of the coffee-ring effect by shape-dependent capillary interactions. Nature 476(7360), 308–311 (2011)
5. Bigioni, T.P., Lin, X.M., Nguyen, T.T., Corwin, E.I., Witten, T.A., Jaeger, H.M.: Kinetically driven self assembly of highly ordered nanoparticle monolayers. Nat. Mater. 5(4), 265–270 (2006)
6. Choi, S., Stassi, S., Pisano, A.P., Zohdi, T.I.: Coffee-ring effect-based three dimensional patterning of micro/nanoparticle assembly with a single droplet. Langmuir 26(14), 11690–11698 (2010)
7. Zhuang, J.L., Zhang, Y., Liu, X.Y., Wang, C., Mao, H.L., Du, X., Tang, J.: Edge enriched self-assembly of Au nanoparticles: Coffee-ring effect during microcontact printing via agarose stamps. Appl. Surf. Sci. 469, 90–97 (2019)
8. Saroj, S.K., Panigrahi, P.K.: Magnetic suppression of the coffee ring effect. J. Magn. Magn. Mater. 513, 167199 (2020)
9. Islam, S., Velev, O.D.: Mechanism and control of "coffee-ring erosion" phenomena in structurally colored ionomer films. Soft Matter 16(11), 2683–2694 (2020)
10. Whitby, C.P., Hermant, A.: Concentration of deposit patterns by nanoparticles modified with short amphiphiles. Colloids Surf. A Physicochem. Eng. Asp. 594, 124648 (2020)
11. Yang, Q., Lv, C., Hao, P., He, F., Ouyang, Y., Niu, F.: Air bubble-triggered suppression of the coffee-ring effect. Colloid Interface Sci. Commun. 37, 100284 (2020)
12. Maenosono, S., Dushkin, C.D., Saita, S., Yamaguchi, Y.: Growth of a semiconductor nanoparticle ring during the drying of a suspension droplet. Langmuir 15(4), 957–965 (1999)

13. Kshirsagar, A., Pickering, S., Xu, J., Ruzyllo, J.: Light emitting diodes formed using mist deposition of colloidal solution of CdSe nanocrystalline quantum dots. ECS Trans. 35(18), 71 (2011)
14. Kshirsagar, A., Jiang, Z., Pickering, S., Xu, J., Ruzyllo, J.: Formation of Photo-Luminescent Patterns on Paper Using Nanocrystalline Quantum Dot Ink and Mist Deposition. ECS J. Solid State Sci. Technol. 2(5), R87 (2013)
15. Yakhno, T.A.: Salt-induced protein phase transitions in drying drops. J. Colloid Interface Sci. 318(2), 225–230 (2008)
16. Yakhno, T.A., Yakhno, V.G., Sanin, A.G., Sanina, O.A., Pelyushenko, A.S.: Protein and salt: Spatiotemporal dynamics of events in a drying drop. Tech. Phys. 49(8), 1055–1063 (2004)
17. Tarasevich, Y.Y., Pravoslavnova, D.M.: Drying of a multicomponent solution drop on a solid substrate: Qualitative analysis. Tech. Phys. 52(2), 159–163 (2007)
18. Sefiane, K.: On the formation of regular patterns from drying droplets and their potential use for bio-medical applications. J. Bionic. Eng. 7(4), S82–S93 (2010)
19. Trantum, J.R., Wright, D.W., Haselton, F.R.: Biomarker-mediated disruption of coffee-ring formation as a low resource diagnostic indicator. Langmuir 28(4), 2187–2193 (2012)
20. Yakhno, T.A., Sanin, A.A., Ilyazov, R.G,. Vildanova, G.V., Khamzin, R.A., Astascheva, N.P., Markovsky, M.G., Bashirov, V.D., Yakhno, V.G.: Drying drop technology as a possible tool for detection leukemia and tuberculosis in cattle. J. Biomed. Sci. Eng. 8(01), 1 (2015)
21. Devineau, S., Anyfantakis, M., Marichal, L., Kiger, L., Morel, M., Rudiuk, S., Baigl, D.: Protein adsorption and reorganization on nanoparticles probed by the coffee-ring effect: application to single point mutation detection. J. Am. Chem. Soc. 138(36), 11623–11632 (2016)
22. Sempels, W., De Dier, R., Mizuno, H., Hofkens, J., Vermant, J.: Auto-production of biosurfactants reverses the coffee ring effect in a bacterial system. Nat. Commun. 4(1), 1–8 (2013)
23. Kasyap, T.V., Koch, D.L., Wu, M.: Bacterial collective motion near the contact line of an evaporating sessile drop. Phys. Fluids 26(11), 111703 (2014)
24. Ranjbaran, M., Datta, A.K.: Retention and infiltration of bacteria on a plant leaf driven by surface water evaporation. Phys. Fluids 31(11), 112106 (2019)
25. Poulichet, V., Morel, M., Rudiuk, S., Baigl, D.: Liquid-liquid coffee-ring effect. J. Colloid Interface Sci. 575, 370–375 (2020)
26. Calvert, P.: Inkjet printing for materials and devices. Chem. Mater. 13(10), 3299–3305 (2001)
27. De Gans, B.J., Duineveld, P.C., Schubert, U.S.: Inkjet printing of polymers: state of the art and future developments. Adv. Mater. 16(3), 203–213 (2004)
28. Park, J., Moon, J.: Control of colloidal particle deposit patterns within picoliter droplets ejected by ink-jet printing. Langmuir 22(8), 3506–3513 (2006)
29. Tekin, E., Smith, P.J., Schubert, U.S.: Inkjet printing as a deposition and patterning tool for polymers and inorganic particles. Soft. Matter. 4(4), 703–713 (2008)
30. Perelaer, J., Schubert, U.S.: Novel approaches for low temperature sintering of inkjet-printed inorganic nanoparticles for roll-to-roll (R2R) applications. J. Mater. Res. 28(4), 564 (2013)
31. Kuang, M., Wang, L., Song, Y.: Controllable printing droplets for high-resolution patterns. Adv. Mater. 26(40), 6950–6958 (2014)
32. Bridonneau, N., Mattana, G., Noel, V., Zrig, S., Carn, F.: Morphological Control of Linear Particle Deposits from the Drying of Inkjet-Printed Rivulets. J. Phys. Chem. Lett. 11(12), 4559–4563 (2020)
33. Morinaga, K., Oikawa, N., Kurita, R.: Emergence of different crystal morphologies using the coffee ring effect. Sci. Rep. 8(1), 1–10 (2018)
34. Baek, J.M., Yi, C., Rhee, J.Y.: Central spot formed in dried coffee-water-mixture droplets: Inverse coffee-ring effect. Curr. Appl. Phys. 18(4), 477–483 (2018)
35. Lian, H., Qi, L., Luo, J., Zhang, R., Hu, K.: Uniform droplet printing of graphene micro-rings based on multiple droplets overwriting and coffee-ring effect. Appl. Surf. Sci. 499, 143826 (2020)
36. Zhang, D., Gao, B., Chen, Y., Liu, H.: Converting colour to length based on the coffee-ring effect for quantitative immunoassays using a ruler as readout. Lab Chip 18(2), 271–275 (2018)
37. Miller, J.B., Usselman, A.C., Anthony, R.J., Kortshagen, U.R., Wagner, A.J., Denton, A.R., Hobbie, E.K.: Phase separation and the 'coffee-ring' effect in polymernanocrystal mixtures. Soft Matter 10(11), 1665–1675 (2014)
38. Yu, Y., Zhu, H., Frantz, J.M., Reding, M.E., Chan, K.C., Ozkan, H.E.: Evaporation and coverage area of pesticide droplets on hairy and waxy leaves. Biosyst. Eng. 104(3), 324–334 (2009)
39. Brutin, D., Sobac, B., Loquet, B., Sampol, J.: Pattern formation in drying drops of blood. J. Fluid. Mech. 667, 85 (2011)
40. Brutin, D., Sobac, B., Nicloux, C.: Influence of substrate nature on the evaporation of a sessile drop of blood. J. Heat. Transfer. 134(6), (2012)
41. Wen, J.T., Ho, C.M., Lillehoj, P.B.: Coffee ring aptasensor for rapid protein detection. Langmuir 29(26), 8440–8446 (2013)
42. Li, Q., Zhu, Y.T., Kinloch, I.A., Windle, A.H.: Self-organization of carbon nanotubes in evaporating droplets. J. Phys. Chem. B 110(28), 13926–13930 (2006)

43. Kimura, M., Misner, M.J., Xu, T., Kim, S.H., Russell, T.P.: Long-range ordering of diblock copolymers induced by droplet pinning. Langmuir 19(23), 9910–9913 (2003)
44. Erbil, H.Y.: Evaporation of pure liquid sessile and spherical suspended drops: A review. Adv. Colloid Interface Sci. 170(1-2), 67–86 (2012)
45. Mampallil, D., Eral, H.B.: A review on suppression and utilization of the coffee-ring effect. Adv. Colloid Interface Sci. 252, 38–54 (2018)
46. Crivoi, A., Duan, F.: Three–dimensional Monte Carlo model of the coffee-ring effect in evaporating colloidal droplets. Sci. Rep. 4, 4310 (2014)
47. Kim, H.S., Park, S.S., Hagelberg, F.: Computational approach to drying a nanoparticle-suspended liquid droplet. J. Nanopart. Res. 13(1), 59–68 (2011)
48. Crivoi, A., Duan, F.: Amplifying and attenuating the coffee-ring effect in drying sessile nanofluid droplets. Phys. Rev. E 87(4), 042303 (2013)
49. Crivoi, A., Duan, F.: Effect of surfactant on the drying patterns of graphite nanofluid droplets. J. Phys. Chem. B 117(19), 5932–5938 (2013)
50. Crivoi, A., Duan, F.: Elimination of the coffee-ring effect by promoting particle adsorption and long-range interaction. Langmuir 29(39), 12067–12074 (2013)
51. Bhardwaj, R., Fang, X., Attinger, D.: Pattern formation during the evaporation of a colloidal nanoliter drop: a numerical and experimental study. New J. Phys. 11(7), 075020 (2009)
52. Xu, T., Lam, M.L., Chen, T.H.: Discrete element model for suppression of coffee-ring effect. Sci. Rep. 7, 42817 (2017)
53. Yang, J., Kim, H., Lee, C., Kim, S., Wang, J., Yoon, S., Kim, J.: Phase-field modeling and computer simulation of the coffee-ring effect. Theor. Comput. Fluid. Dyn. 34(5), 679–692 (2020)

Figures

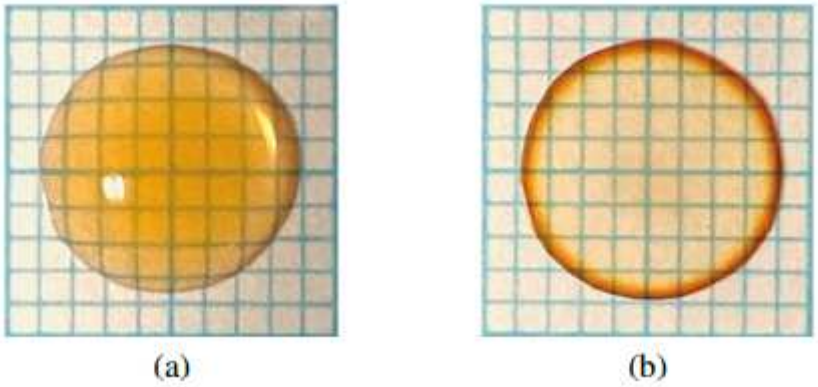

Figure 1

Coffee droplet on a transparent film on a grid paper (a) before and (b) after evaporation.

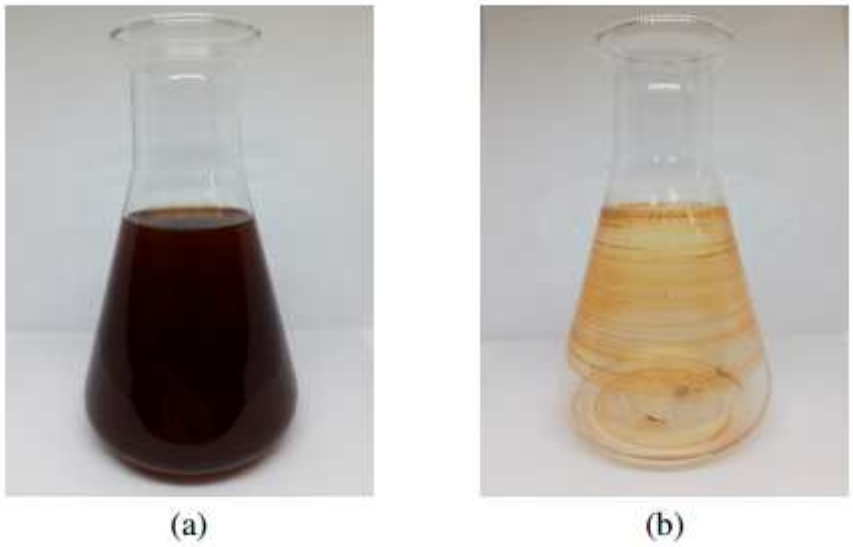

Figure 2

Making coffee angel rings in a conical flask: (a) Coffee solution contained in a conical flask and (b) Coffee angel rings made after evaporation.

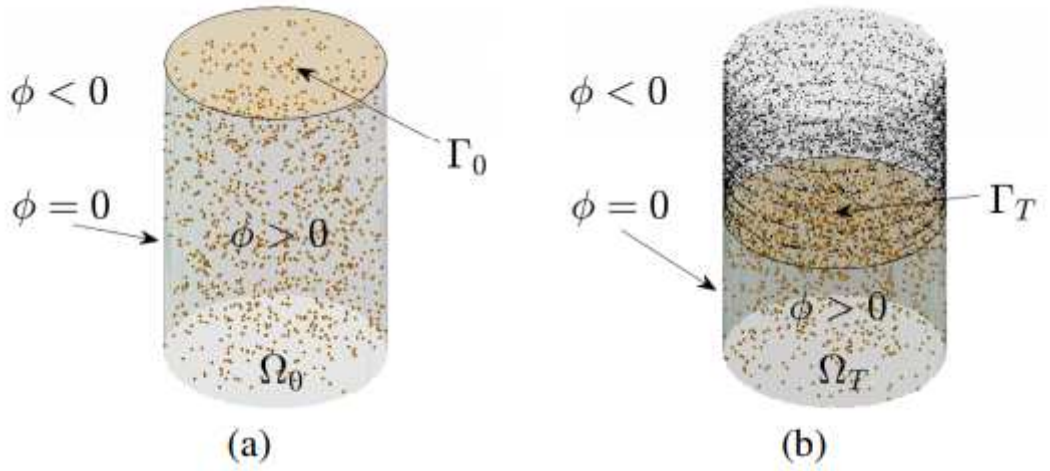

Figure 3

Schematic illustration of the liquid domain Ωt over time at (a) t = 0 and (b) t = T where T is a certain time. Note that the coloured surface represents the top-level surface Γt

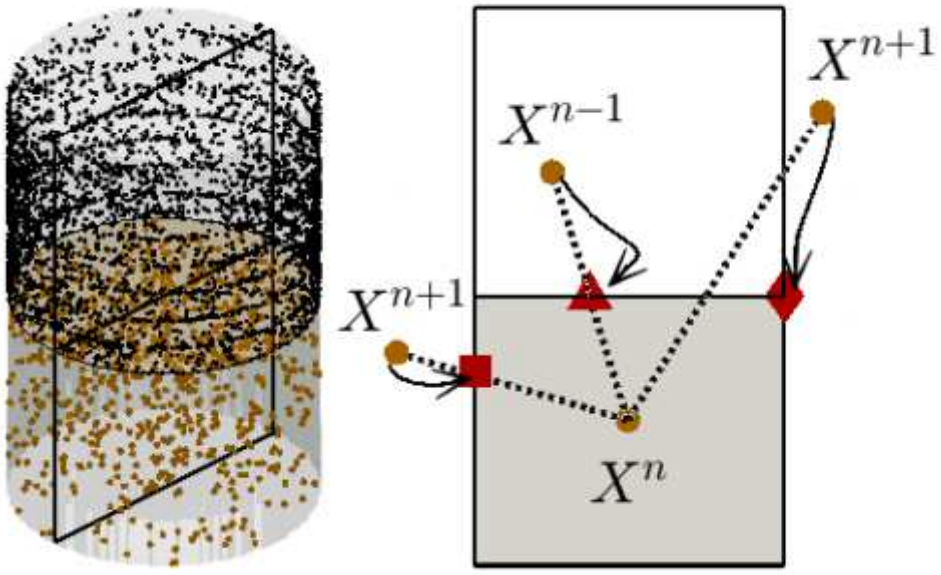

Figure 4

Schematic representation of pinning process

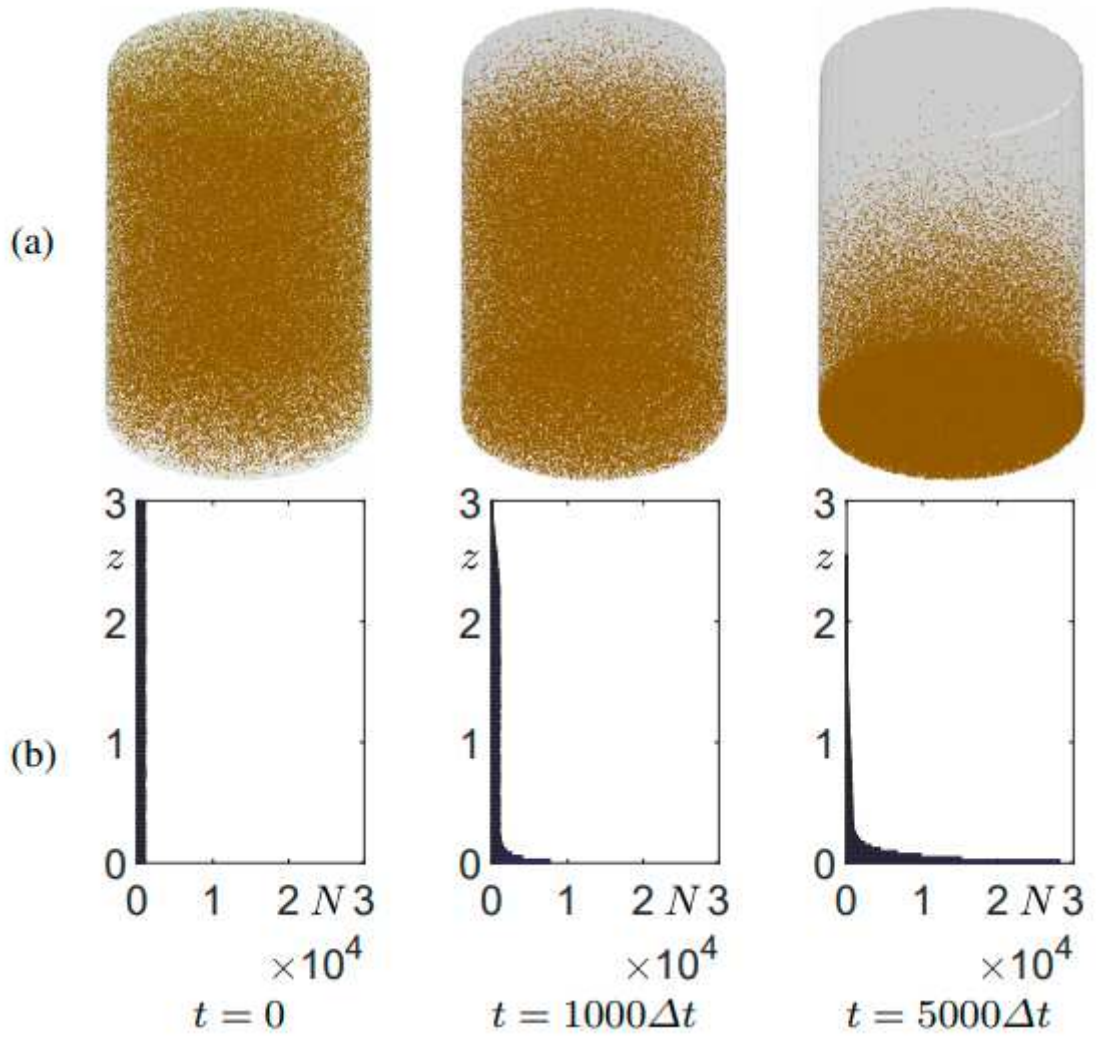

Figure 5

(a) Evolution of particles in a cylindrical container without evaporation. (b) Histograms of particle number with respect to height at the corresponding times

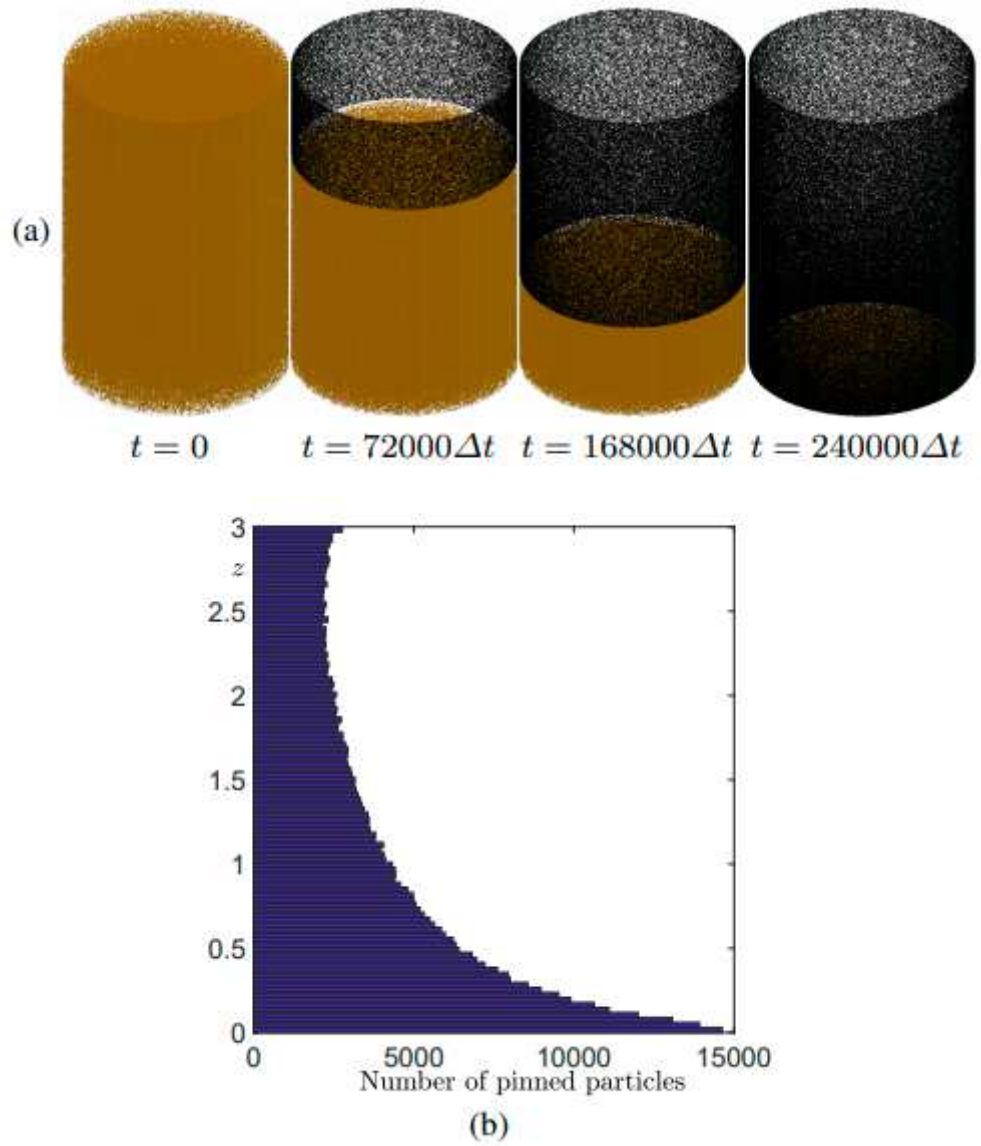

Figure 6

(a) Evolution of particles in a cylindrical container. (b) Histogram of pinned particles with respect to height at final time t = 240000Δt.

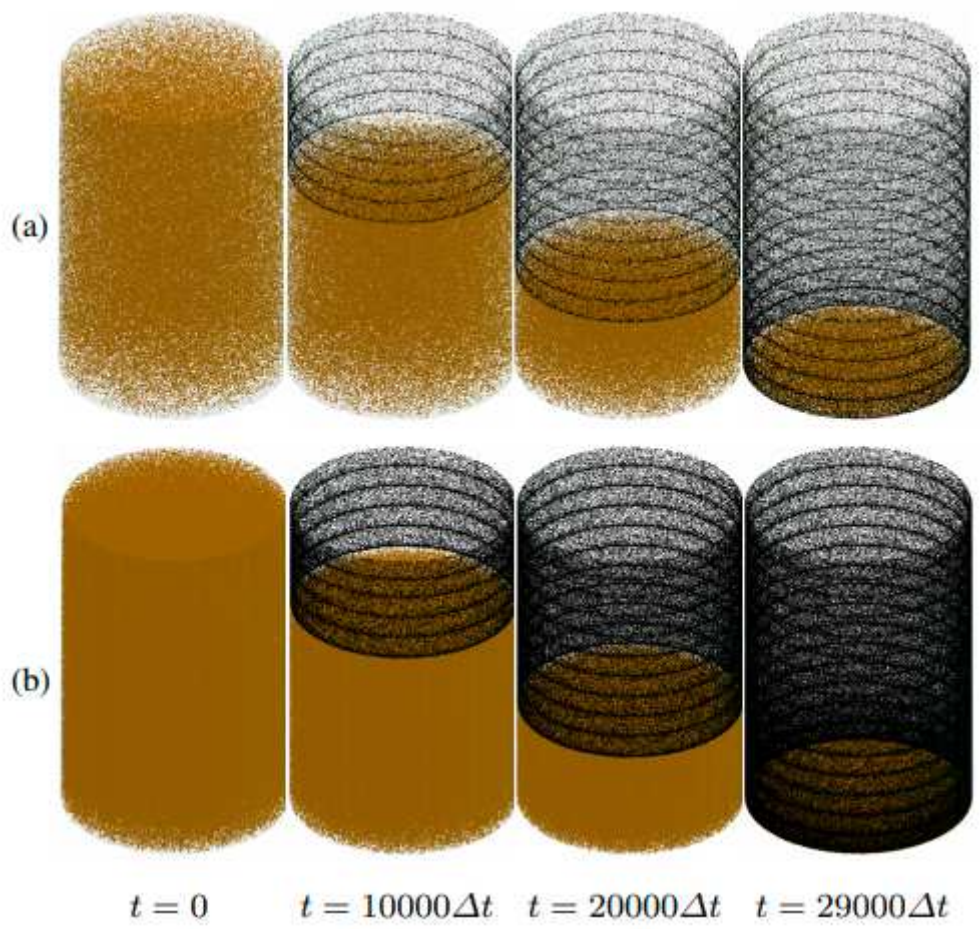

Figure 7

Evolution of particles on the time-dependent evaporation rate in a cylindrical container: the number of particles is (a) 100000 and (b) 500000.

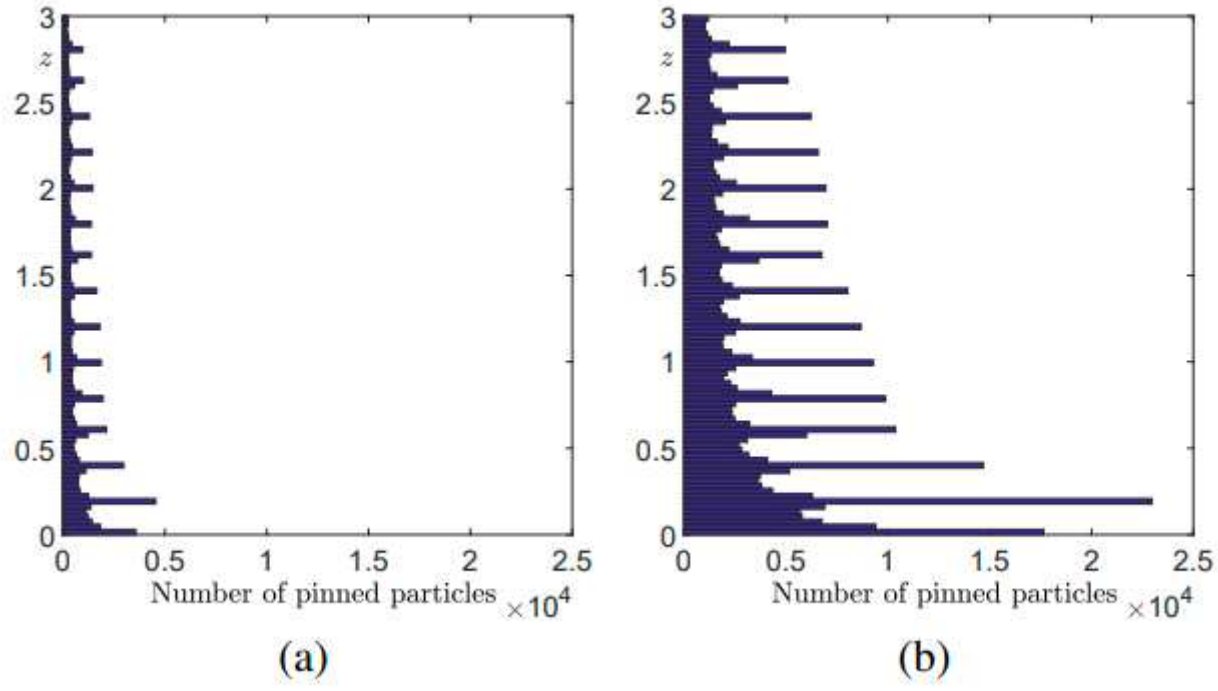

Figure 8

Histogram of particles with respect to height at final time t = 29084Δt. The number of particles is (a) 100000 and (b) 500000

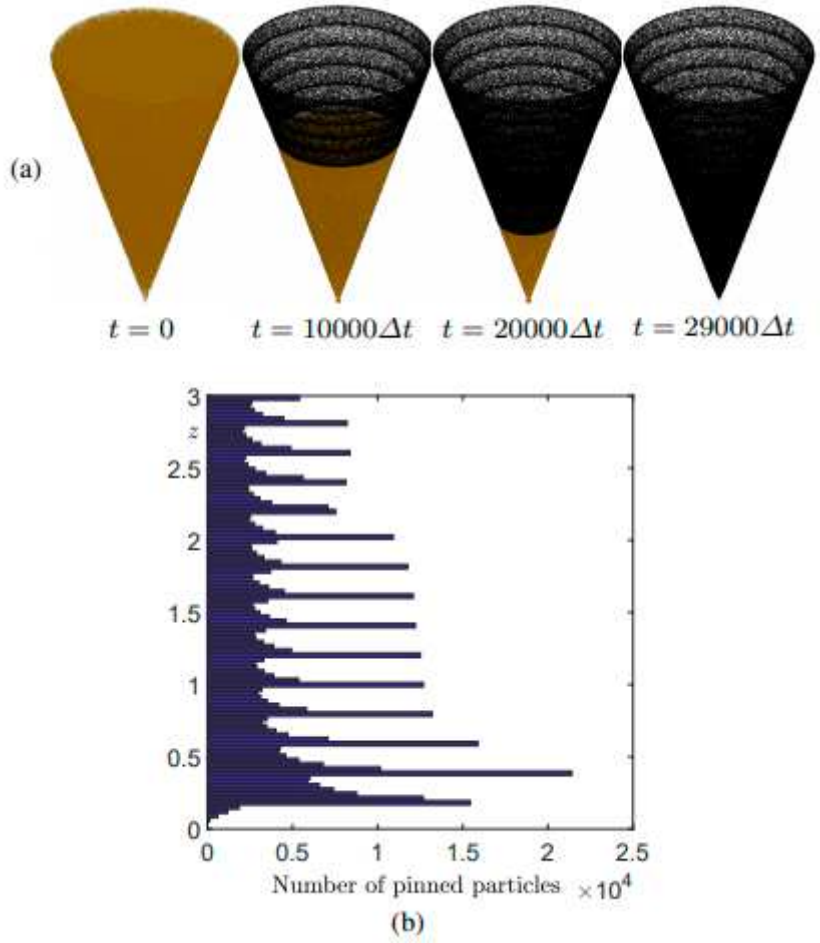

Figure 9

(a) Evolution of particles on the time-dependent evaporation rate in a conical container. (b) Histogram of particles with respect to height at final time t = 29084Δt

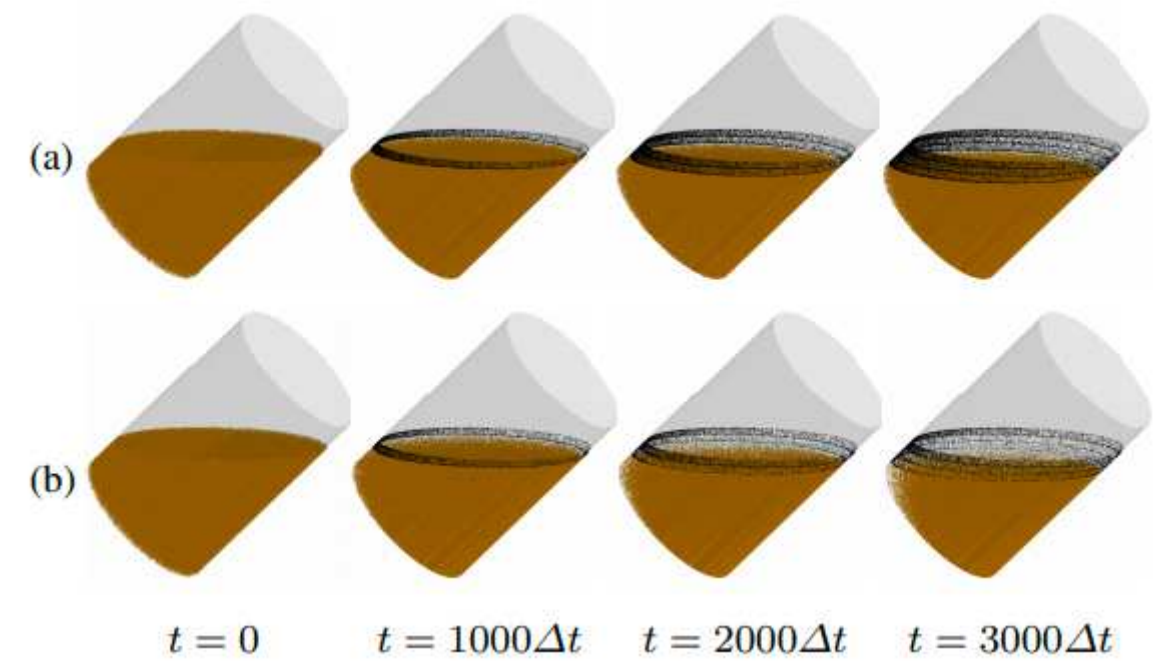

Figure 10

Effect of gravitational parameter on the formation of coffee ring with (a) g = 2 and (b) g = 4.

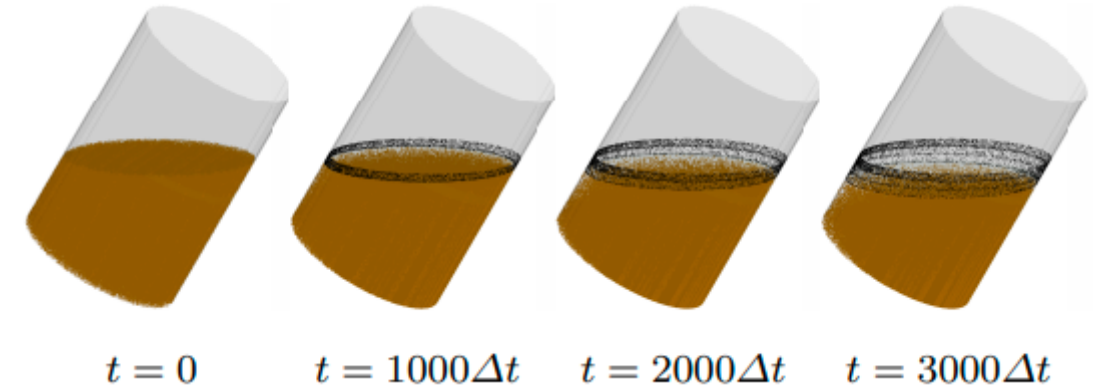

Figure 11

1 Evolution of particles on a time-dependent evaporation rate in a 30□ tilted cylinder.

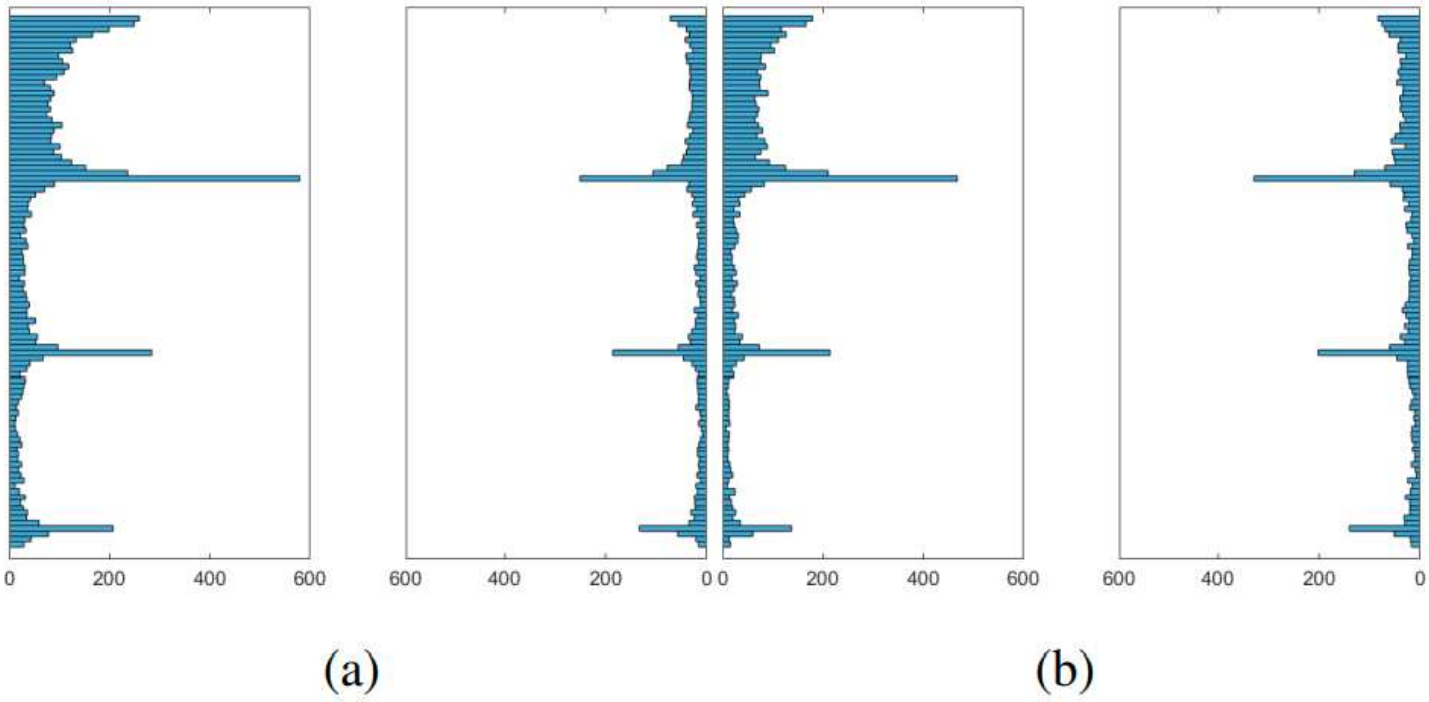

Figure 12

Histograms of number of pinned particles with respect to height at final time t = 3000Δt in (a) 45° tilted and (b) 30° tilted cylinders